Ecosystems
https://doi.org/10.1007/s10021-024-00936-7

CO_2 and CH_4 Concentrations in Headwater Wetlands Influenced by Morphology and Changing Hydro-Biogeochemical Conditions

Carla López Lloreda,[1]* James Maze,[2,6] Katherine Wardinski,[3] Nicholas Corline,[4] Daniel McLaughlin,[4] C. Nathan Jones,[5] Durelle Scott,[3] Margaret Palmer,[2] and Erin R. Hotchkiss[1]

[1]*Department of Biological Sciences, Virginia Polytechnic Institute and State University, Derring Hall 2125, 926 West Campus Drive, Blacksburg, Virginia 24061, USA;* [2]*Department of Entomology, Plant Sciences Building, University of Maryland, 4291 Fieldhouse Dr, College Park, Maryland 20742, USA;* [3]*Biological Systems Engineering, Virginia Polytechnic Institute and State University, Seitz Hall 200, 155 Ag Quad Lane, Blacksburg, Virginia 24061, USA;* [4]*Department of Forest Resources and Environmental Conservation, Virginia Polytechnic Institute and State University, Cheatham Hall 313, 310 West Campus Drive, Blacksburg, Virginia 24061, USA;* [5]*Biology Department, University of Alabama, Science and Engineering Complex, 1325 Hackberry Ln, Tuscaloosa, Alabama 35401, USA;* [6]*Department of Geography, University of Oregon, Condon Hall 1321 Kincaid St., Eugene, OR 97401, USA*

Abstract

Headwater wetlands are important sites for carbon storage and emissions. While local- and landscape-scale factors are known to influence wetland carbon biogeochemistry, the spatial and temporal heterogeneity of these factors limits our predictive understanding of wetland carbon dynamics. To address this issue, we examined relationships between carbon dioxide (CO_2) and methane (CH_4) concentrations with wetland hydrogeomorphology, water level, and biogeochemical conditions. We sampled water chemistry and dissolved gases (CO_2 and CH_4) and monitored continuous water level at 20 wetlands and co-located upland wells in the Delmarva Peninsula, Maryland, every 1–3 months for 2 years. We also obtained wetland hydrogeomorphologic metrics at maximum inundation (area, perimeter, and volume). Wetlands in our study were supersaturated with CO_2 (mean = 315 μM) and CH_4 (mean = 15 μM), highlighting their potential role as carbon sources to the atmosphere. Spatial and temporal variability in CO_2 and CH_4 concentrations was high, particularly for CH_4, and both gases were more spatially variable than temporally. We found that groundwater is a potential source of CO_2 in wetlands and CO_2 decreases with increased water level. In contrast, CH_4 concentrations appear to be related to substrate and nutrient availability and to drying patterns over a longer temporal scale. At the landscape scale, wetlands with higher perimeter:area ratios and wetlands with higher height above the nearest drainage had higher CO_2 and CH_4 concentrations. Understanding the variability of CO_2 and CH_4 in wetlands, and how these might change with changing environmental conditions and across different wetland types, is critical to understanding

Received 18 March 2024; accepted 9 September 2024

Supplementary Information: The online version contains supplementary material available at https://doi.org/10.1007/s10021-024-00936-7.

Author Contributions Author Contributions DM, MP, ERH, DS, and CNJ conceived the study and obtained funding for this work. JM led fieldwork with support from CLL, KW, and NC. CLL, CNJ, JM, and NC obtained and processed data. CLL analyzed the data and wrote the manuscript, with substantial support from ERH and input from all authors. All authors provided feedback and edits to the manuscript and approved the submitted version.

*Corresponding author; e-mail: carlalopez@vt.edu

Published online: 01 October 2024

the current and future role of wetlands in the global carbon cycle.

Key words: Headwater wetlands; Greenhouse gases; CO_2; CH_4; Spatiotemporal variability; Carbon biogeochemistry; Surface water groundwater; Hydrologic variability.

Highlights

- Groundwater seems to be an important source of CO_2 to these small wetlands
- CH_4 was governed by changing substrate availability and associated redox conditions
- Wetlands with higher perimeter:area and height above nearest drainage had higher CO_2 and CH_4 concentrations

Introduction

Wetlands play an important role in the global carbon (C) cycle through their contribution to C storage, carbon dioxide (CO_2) and methane (CH_4) emissions, and lateral transport of C to downstream ecosystems (Li and others 2022). While the C stored in wetland soils is substantial, emissions of CO_2 and CH_4 from wetland surfaces may be enough to offset the soil C storage pool in some ecosystems (Rosentreter and others 2021). Further, global wetland soil and plant C storage are relatively stable over time (Webb and others 2019), but CO_2 and CH_4 dynamics are more variable and have been increasing over the past decade (Peng and others 2022). Variability in CO_2 and CH_4 is due to the many sources and processes regulating CO_2 and CH_4 in wetlands. Thus, understanding the variability and associated environmental and biogeochemical factors influencing wetland CO_2 and CH_4 is critical to improving our understanding of the role of wetlands in the global C cycle and wetland responses to a changing climate.

Small, headwater wetlands, sometimes called geographically isolated wetlands, are depressional wetlands surrounded by uplands (Tiner 2003). They occur across different regions in the USA and include the Prairie Pothole wetlands in the Midwest, vernal pools in New England and California, Carolina Bays in the Southeast, and Delmarva Bays in the mid-Atlantic, the latter of which are the focus of this study. Small, shallow, depressional wetlands represent a significant area of wetland-rich regions and provide ecosystem services such as sediment and nutrient retention, flood attenuation, and baseflow contribution during low precipitation periods (Marton and others 2015). However, they face increasing challenges as they lose federal protections; thus, quantifying their contributions to regional and global ecosystem services is of critical importance (Creed and others 2017).

In small wetlands, CO_2 and CH_4 concentrations in surface water are usually high and supersaturated with respect to the atmosphere (Holgerson and Raymond 2016) but are often still excluded from landscape- and global-scale C budgets. Due to high connectivity with the terrestrial landscape and more direct inputs of organic matter, small wetlands can be biogeochemical hotspots with a disproportionate contribution to C fluxes than their larger counterparts (Holgerson 2015). Further, upscaling of CO_2 and CH_4 contributions from wetlands frequently leaves out smaller water bodies, due to its dependence on using satellite imagery which is biased toward larger wetlands (Hondula and others 2021a). In more recent upscaling efforts, small water bodies ($< 1000\ m^2$) were found to contribute approximately 15.1% of CO_2 and 40.6% of CH_4 freshwater global emissions (Holgerson and Raymond 2016).

The upscaling and global models of carbon emissions rely on a limited understanding of CO_2 and CH_4 variability, which can be influenced by many factors (Saunois and others 2020). The production of CO_2 and CH_4 is influenced by physicochemical and biogeochemical conditions such as oxygen availability, terminal electron acceptors (TEAs), nutrients, and dissolved organic matter (DOM) concentrations (Bridgham and others 2006). Oxygen availability, which decreases with water saturation and inundation, influences the balance between the consumption and production of CO_2 and CH_4 in wetlands (Maietta and others 2020). Under saturated conditions, the wetland environment becomes anoxic, and these conditions favor CH_4 production after other TEAs (O_2, NO_3^-, Mn^{4+}, Fe^{3+}, SO_4^{2-}) have been used. While CH_4 production under strictly anoxic conditions has been the established paradigm, CH_4 production under oxic conditions is increasingly being documented and supported by experimental evidence (Angle and others 2017). Similarly, the oxidation of organic matter into CO_2 occurs at a faster rate in the presence of oxygen, while decomposition progresses more slowly under anoxic conditions. The availability of organic matter also influences concentrations of CO_2 and CH_4 as a variety of DOM substances, such as acetate, serve as a substrate for

the reactions of CH_4 and CO_2 production (Cozannet and others 2023). CH_4 production can also use CO_2 as a substrate in hydrogenotrophic methanogenesis. Thus, an increase in DOM usually leads to an increase in CH_4 and CO_2 concentrations (Nikolenko and others 2019). While acetoclastic methanogenesis is considered the most common pathway in wetlands, an array of other substrates can also be used to produce CH_4. Ultimately, the variability in environmental and biogeochemical conditions such as oxygen availability, DOM and TEA concentrations, and other environmental factors (hydrology, climate, geology) results in CO_2 and CH_4 dynamics that are highly variable, and because of the many production pathways of CH_4, they remain harder to generalize and predict than CO_2 (Bridgham and others 2013).

Beyond the inherent variability in CO_2 and CH_4 cycling, smaller wetlands tend to experience variable water level regimes and hydrologic connections, with associated variability in water sources and their biogeochemical processes, making them more hydrologically variable than other wetland types (Marton and others 2015). Sources of CO_2 and CH_4 can vary as wetlands connect with different parts of the landscape across changing seasonal and event-based hydrologic conditions, including fluctuating contributions from groundwater (Rudolph and others 2020). Changing hydrologic connectivity among wetlands and with the larger fluvial network can also control CO_2 and CH_4 dynamics by transporting dissolved CO_2 and CH_4 into and out of wetlands (Abril and Borges 2019; Bretz and others 2021). In wetlands that experience greater hydrologic variability and frequent wet-dry cycles, microbial communities tend to be more diverse and adaptable than in soils that experience more stable conditions (Peralta and others 2014). Specifically, soil microbial communities, including methanogens and methanotrophic bacteria responsible for CO_2 and CH_4 production and consumption, are influenced by water level both below and above ground surface and inundation frequency (Maietta and others 2020). Changing water level and inundation frequency can therefore result in significant changes in CO_2 and CH_4 production and consumption. For example, in tropical wetlands with seasonally changing hydrology, total annual CH_4 emissions were higher than in permanently flooded tropical wetlands (Mitsch and others 2010). Changing hydrology plays a major role in influencing biogeochemical dynamics in wetlands, but the extent to which it controls the temporal and spatial variability in greenhouse gases in small, hydrologically dynamic wetlands is still relatively uncharacterized.

This study aimed to quantify the variability and associated variables influencing CO_2 and CH_4 concentrations in surface water across 20 small, headwater wetlands of varying hydrogeomorphological characteristics and inundation regimes in the Delmarva Peninsula in the Mid-Atlantic region of the USA. We ask: (1) What is the magnitude and variability of CO_2 and CH_4 concentrations among headwater wetlands and across seasons? and (2) What factors are associated with CO_2 and CH_4 concentrations and variability in temperate headwater wetlands? We hypothesized that there would be high spatial and temporal variability in surface water CO_2 and CH_4 concentrations, particularly for CH_4, and that this variability would be largely associated with the hydrologic (water level) variation of these wetlands, both due to wet-dry cycles and seasonal drying and wetting up periods. Further, we expected concentrations of CO_2 and CH_4 to be correlated with substrate availability (that is, organic matter), oxygen concentrations, and redox-sensitive ions. At the landscape scale, we expected smaller wetlands to have higher concentrations of CO_2 and CH_4.

Methods

Study Sites

Our wetland study sites are located in the Upper Choptank and Tuckahoe River watersheds in the Delmarva Peninsula, Maryland, USA (Figure 1). The Delmarva Peninsula is a low-relief landscape with extensive depressional wetlands surrounded by forested wetland flats and uplands (Fenstermacher and others 2014). The wetlands included in this study represent a range of wetland characteristics in this landscape, including varying morphology, size, and dominant vegetation (Table 1). For example, some wetlands are depressional, bowl-shaped with forested vegetation, while others are flat and expansive with emergent vegetation (Figure 1). However, sites with emergent vegetation have low representation in our dataset (n = 4) and we thus did not assess the role of vegetation in mediating CO_2 and CH_4 dynamics, although we recognize that vegetation type influences CO_2 and CH_4 dynamics in wetlands (McInerney and Helton 2016; Sharp and others 2024). In the forested wetlands, the dominant vegetation is *Acer rubrum* (Red maple), *Liquidambar styraciflua* (Sweetgum), *Ilex opaca* (American Holly), and *Quercus rubra* (Northern Red Oak) and vegetation is sparse within

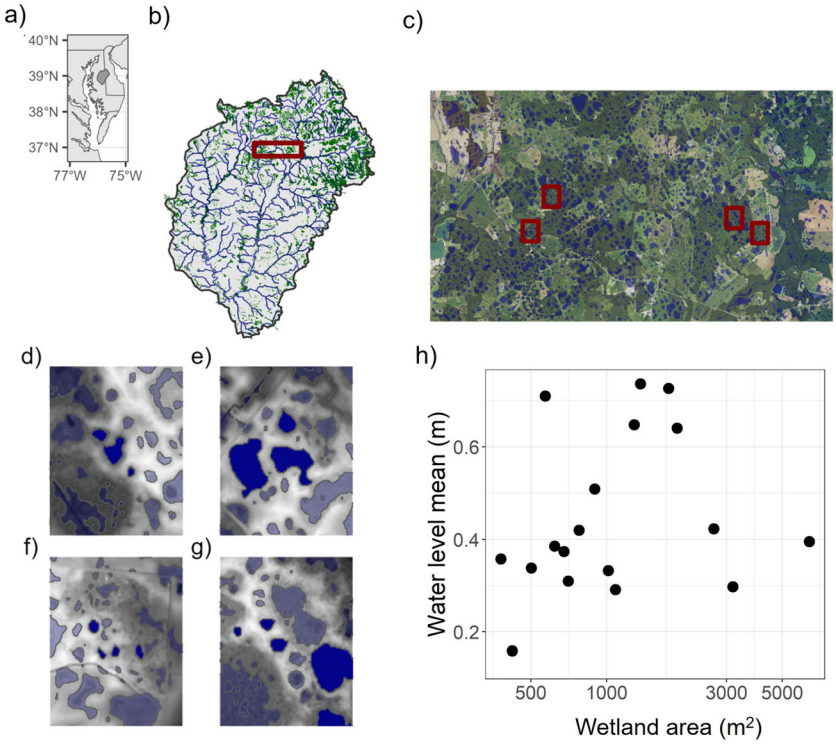

Figure 1. Map of the Delmarva Peninsula and location and physical characteristics of our study wetlands. Map of the Eastern Shore, USA (**a**), with an inset of the Delmarva Peninsula and the Greensboro Watershed (**b**). We also show the location of the different wetland complexes **c** with a zoomed in view of each wetland complex and their corresponding wetlands at maximum inundation (**d–g**). Darker-colored wetlands indicate the wetlands in our study (**d–g**). Water level average and wetland area of our study wetlands, which are generally small, shallow wetlands (**h**).

the wetland inundated area. In emergent wetlands, the vegetation distribution is patchy and includes zones of open water, the sedge *Carex,* and other marsh species. The wetlands experience partial to total canopy cover from May through September, followed by leaf off in October. Study wetlands were clustered within four distinct geographic areas, hereafter called wetland complexes: Jackson Lane (JL), Tiger Paw (TP), Baltimore Corner (BC), and Jones Road (JR; Figure 1d–g). Within each complex, intermittent surface connectivity occurs at most wetlands; however, some sites experience no surface connectivity and are considered isolated.

The wetlands in this landscape have distinct inundation patterns, with increases in surface water levels during late fall and winter and an evapotranspiration-driven drying period during late spring and summer (McDonough and others 2015; Lee and others 2020). Water level varies significantly among Delmarva wetlands, but seasonal patterns are similar (Stewart and others 2023). Seasonal hydrologic patterns are disrupted by localized rain events, particularly tropical storms and convective storms during the summer and fall. During high water levels and inundated conditions, approximately half of these wetlands experience ephemeral surface water connections, the degree to which depends on surrounding landscape topology (McDonough and others 2015). The groundwater table and its interaction with the wetland represent a gradient of flowthrough, recharge, or discharge conditions and can also shift between these conditions (Phillips and Shedlock 1993).

Wetland Characterization: Hydrogeomorphic Variables

We characterized wetland hydrogeomorphology using metrics of wetland area, wetland perimeter, wetland volume, and height above nearest drainage (HAND) derived from a terrain analysis similar to Jones and others (2018). Briefly, this analysis was conducted on a high-resolution LiDAR-based digital elevation model (DEM) with a resolution of 1 m (Maryland Department of Information Technology 2013). First, we identified internally draining basins within the DEM and then the maximum inundation areas within those basins (Le and Kumar 2014). Then, we used the level-set method to quantify both nested and network connectivity of

Table 1. Hydrogeomorphic and Vegetation Characteristics Across Wetlands

Wetland ID	Wetland complex	Wetland area (m^2)	Wetland storage volume (m^3)	Mean elevation (m)	Wetland perimeter (m)	Perimeter: area	Dominant vegetation	Average water level (m)
E1	Baltimore Corner	6410	2825.8	18.3	418	0.19	Emergent	0.5
E4	Baltimore Corner	3182	2020.2	18.1	274	0.09	Emergent	0.3
F4	Baltimore Corner	620	193.3	18.3	120	0.19	Forested	0.4
F8	Baltimore Corner	1766	982	18.5	244	0.14	Forested	0.7
F11	Baltimore Corner	421	50.28	18.8	142	0.34	Forested	0.2
F12	Baltimore Corner	777	298.5	18.3	122	0.16	Forested	0.4
F16	Baltimore Corner	470	125.7	18.7	120	0.25	Forested	0.1
E2	Jackson Lane	3464	904.7	15.5	464	0.13	Emergent	NA
F1	Jackson Lane	379	109.9	15.1	132	0.35	Forested	0.4
F3	Jackson Lane	897	344.9	14.2	168	0.07	Forested	0.4
F10	Jackson Lane	1364	972.2	14.7	174	0.13	Forested	0.7
F15	Jackson Lane	676	334.4	14.8	136	0.2	Forested	0.4
F5	Jones Road	703	129.5	18.7	136	0.19	Forested	0.3
F6	Jones Road	2667	1377.5	18.6	270	0.1	Forested	0.4
F7	Jones Road	1015	339.3	18.8	162	0.16	Forested	0.3
F9	Jones Road	501	158.7	19	112	0.22	Forested	0.3
E3	Tiger Paw	1085	356.1	16	308	0.28	Emergent	0.3
F2	Tiger Paw	569	340.5	16	110	0.19	Forested	0.7
F13	Tiger Paw	1287	849.1	16.1	170	0.13	Forested	0.7
F14	Tiger Paw	1907	904.1	16	212	0.11	Forested	0.6

Site IDs, wetland complex, morphological characteristics, and average water level for our 20 wetlands located in the Delmarva Peninsula, Maryland. Wetland complex refers to the area it is located in. Wetlands within the same wetland complex could experience surface connections, but some sites are considered truly isolated. Wetland morphological variables here were extracted from a digital elevation model (DEM) and represent area, volume, and perimeter at maximum inundation. Mean elevation represents the average elevation across the entire wetland. Average water level was obtained from wells installed in the middle of each wetland. Sites are arranged by corresponding wetland complex and denoted by their site ID in which E is an emergent vegetation wetland and F is a forested vegetation wetland.

wetlands (Wu and others 2019). Finally, we calculated metrics for individual wetlands. A single, site-specific value for wetland area, wetland perimeter, and wetland volume was calculated using maximum inundation extent. HAND was calculated as the elevation difference between wetland and stream network (Rennó and others 2008). All spatial analyses were completed using whitebox tools (Lindsay 2016, Wu and Brown 2022).

Wetland Characterization: Inundation Regimes

To characterize the inundation regimes for the present study sites, we monitored water level from 2020 to 2022 in wells installed in the deepest point of each wetland and in upland wells near each wetland. Wetland wells were augured 50 cm below ground surface. Upland wells were installed roughly 1.5 m away from the wetland edge in the upland area adjacent to wetlands, as defined by

Table 2. Water Chemistry Across Wetlands

Site	Wetland complex	CO_2 (uM)	CH_4 (uM)	Temp (C)	pH	SpC (uS/cm)	DO (mg/L)
E1	Baltimore Corner	128.6 ± 42.6	2.8 ± 4.1	15 ± 6.5	6.8 ± 2.2	29.3 ± 3.6	8.7 ± 1.8
E4	Baltimore Corner	305.3 ± 140.7	4 ± 3	13.9 ± 6.4	6.1 ± 3	35.7 ± 8.5	8 ± 1.4
F11	Baltimore Corner	345 ± 88.3	3.8 ± 4.2	11.2 ± 5.7	3.9 ± 0.5	113.1 ± 89	6.3 ± 4.8
F12	Baltimore Corner	297 ± 123.4	9.9 ± 8.4	13 ± 6	6.8 ± 2.3	37.6 ± 6.1	5.8 ± 2.5
F16	Baltimore Corner	407.6 ± 185.1	6.3 ± 7.1	12.6 ± 6.7	4.3 ± 0.3	62 ± 46	6.1 ± 2
F4	Baltimore Corner	422 ± 77.3	18.2 ± 17.2	12 ± 5.3	4.3 ± 0.3	67 ± 33	4.5 ± 2.2
F8	Baltimore Corner	337.5 ± 83.6	5.2 ± 4.4	11.7 ± 5.6	4.3 ± 0.2	51.9 ± 17	5.9 ± 2.1
E3	Jackson Lane	102.2 ± 36.1	1 ± 0.7	29.2 ± NA	4.8 ± NA	20.1 ± NA	8.4 ± NA
F1	Jackson Lane	689.6 ± 263.9	46.9 ± 32	11.1 ± 4.9	5.9 ± 2	69.5 ± 25.3	2.8 ± 1.7
F10	Jackson Lane	274.3 ± 94.8	2.5 ± 2.3	11.3 ± 6.1	5.9 ± 2	40 ± 38.9	4.8 ± 2.6
F15	Jackson Lane	382.9 ± 170.9	6.2 ± 4.7	11.4 ± 5.8	5.8 ± 2.4	35.8 ± 7.8	3.4 ± 1.8
F3	Jackson Lane	307.3 ± 88.9	4.8 ± 3.6	12.2 ± 5.9	5.5 ± 2.1	39.4 ± 9	4.6 ± 2.5
F5	Jones Road	323.7 ± 63.7	13.7 ± 10.2	13.8 ± 5.7	7.4 ± 2.8	43.7 ± 7.7	5.2 ± 2.6
F6	Jones Road	242 ± 117	10.1 ± 16.5	13.3 ± 5.6	7.5 ± 3	35.9 ± 8.3	6.2 ± 2.9
F7	Jones Road	416.8 ± 116.5	30.2 ± 24	13.1 ± 5.1	7.7 ± 2.9	36 ± 6.2	5 ± 2.3
F9	Jones Road	300.3 ± 49.1	8.8 ± 7.1	13.7 ± 3.1	6.3 ± 2.3	42.5 ± 12.7	4.8 ± 2.5
E2	Tiger Paw	397.5 ± 181.3	1.3 ± 1	14.5 ± 4.1	6.7 ± 2.7	25.1 ± 2.8	6.9 ± 2.2
F13	Tiger Paw	267.9 ± 55.7	19.2 ± 14.9	12.6 ± 4.8	7.8 ± 2.4	27.2 ± 2.2	3.4 ± 1.8
F14	Tiger Paw	375.1 ± 110.2	35.7 ± 27.3	12.9 ± 3.9	6.3 ± 2.1	37.9 ± 5.5	4.5 ± 2.2
F2	Tiger Paw	301.3 ± 94.4	10.7 ± 9.6	12.1 ± 4	6.7 ± 2.1	34.1 ± 11.1	3.3 ± 1.6

Site	Wetland complex	DOC (mg/L)	TDP (ug/L)	TDN (ug/L)	NH_4 (ug/L)	NO_3 (ug/L)
E1	Baltimore Corner	23.9 ± 5.4	16.8 ± 13.6	1003.2 ± 258.5	32.6 ± 25.7	13.4 ± 11.6
E4	Baltimore Corner	30.3 ± 6.8	37.5 ± 20.9	1107.4 ± 375	56 ± 30.6	13.9 ± 14
F11	Baltimore Corner	48.1 ± 18.5	30.2 ± 13.8	1089.5 ± 188	15.4 ± 4	9 ± 1.7
F12	Baltimore Corner	34 ± 9.2	58.2 ± 82.3	1199.3 ± 275.8	64.4 ± 37.5	13.8 ± 11.2
F16	Baltimore Corner	42 ± 15.2	33.5 ± 12.9	1363.8 ± 427.4	21.1 ± 8.1	16.3 ± 15.8
F4	Baltimore Corner	54.4 ± 45.6	40.4 ± 26.3	1198.3 ± 328.1	15.4 ± 3.7	15 ± 13.4
F8	Baltimore Corner	28.6 ± 7.9	28 ± 14.9	1028.6 ± 400.4	25.3 ± 11.8	12 ± 11.9
E3	Jackson Lane	23.4 ± 4.8	24.6 ± 6.4	1194.7 ± 213.9	46.6 ± 16.5	10.2 ± 5.4
F1	Jackson Lane	55.9 ± 10.3	93.8 ± 97.8	2795.5 ± 1772.4	792.5 ± 1266.2	31.1 ± 44.8
F10	Jackson Lane	21.4 ± 4.9	25.5 ± 11.1	898.6 ± 232.4	34.6 ± 26.1	10.9 ± 9.6
F15	Jackson Lane	35.2 ± 7.7	29.8 ± 13.8	1355.7 ± 276.3	156.1 ± 283.7	12.3 ± 10.2
F3	Jackson Lane	31.1 ± 8.7	32 ± 35.3	1078.3 ± 320.9	54.5 ± 76.8	11 ± 9.5
F5	Jones Road	37.6 ± 13.4	46.9 ± 46.5	1277 ± 549	84.1 ± 90.6	13.5 ± 11.5
F6	Jones Road	29.5 ± 12.7	22.2 ± 17.8	957.3 ± 346.6	47.8 ± 42.1	12.9 ± 12.1
F7	Jones Road	32.7 ± 16.4	25.9 ± 16.4	1000.3 ± 371.2	44.5 ± 28.9	13 ± 12
F9	Jones Road	27.1 ± 10.8	35.2 ± 25.4	974.4 ± 417.1	110.8 ± 169.6	12.9 ± 12
E2	Tiger Paw	23.1 ± 6.1	26.5 ± 33.4	795.1 ± 214.2	26.5 ± 22	14 ± 11.3
F13	Tiger Paw	25.5 ± 5.9	23.6 ± 13.1	790.1 ± 176.2	33.8 ± 29.8	12.8 ± 12.1
F14	Tiger Paw	33.7 ± 9.8	18.5 ± 9.2	953.3 ± 213.9	35.7 ± 33.9	13 ± 10.6
F2	Tiger Paw	34.5 ± 11.4	63.3 ± 78.5	1345.9 ± 692.6	237.6 ± 499.9	15.2 ± 12.9

Mean ± standard deviation of water chemistry and physicochemical parameters for 20 wetlands in the Delmarva Peninsula, Maryland.Sites are arranged by corresponding wetland complex and denoted by their site ID in which E is an emergent vegetation wetland and F is a forested vegetation wetland.
SpC specific conductivity, DO dissolved oxygen concentrations, DOC dissolved organic carbon,TDP total dissolved phosphorus, TDN total dissolved nitrogen.Sites with NA in the standard deviation with only one measurement.

both topography and changes in vegetation. Wells were hand augered to depth of 2–4 m and were screened to near the surface. We installed pressure transducers (Onset HOBOs U20-001–01 and U20L-04; Onset Computer Co., Bourne, MA, USA) which recorded data every 15 min near the bottom of the wetland and upland wells. We corrected the pressure from the well logger with the pressure from an atmospheric pressure sensor located outside of the well (Onset HOBOs U20-001–01 and U20L-04; Onset Computer Co., Bourne, MA, USA) to obtain an atmospheric-corrected pressure and convert into water level relative to ground surface.

Synoptic Sampling: Surface Water and Groundwater Collection

We sampled surface and groundwater at 20 wetland sites 11 times from November 2020 to December 2022, every 1–3 months. Surface water samples were collected from the center of each wetland using a bucket attached to a long pole to gently bring water to the wetland's edge for processing (see below) to minimize sediment disturbance or reaeration. When the wetland was dry, we sampled from the well located near the middle of the wetland. To sample groundwater, we pumped water from each upland well using a peristaltic pump (Geopump Peristaltic DC pump, Geotech, Denver, CO, USA). Wells were purged for two to five minutes or until dry and after purging, wells were left to rebound before sampling. We then used the pump at the lowest rate to limit degassing and slowly collected groundwater into the sampling bucket. During surface water and groundwater sampling, we measured dissolved oxygen (DO), pH, water temperature, and conductivity using a YSI ProDSS handheld meter (YSI, Yellowsprings, OH, USA) after water was removed for CO_2 and CH_4 samples and other water chemistry analyses.

Greenhouse Gas and Water Chemistry Sampling and Analysis

We sampled dissolved CO_2 and CH_4 using the headspace equilibration method (for example, Bansal and others 2023). A 20 ml bubble-free sample of surface water or groundwater from the sampling bucket was pulled into a 60-mL syringe, and 20 mL of headspace as ambient air was added to each syringe before closing the syringe off from the atmosphere with a stopcock. The water samples were then equilibrated by shaking for 2–3 min. Headspace samples were then transferred to sealed 20-ml glass vials filled with ambient air while simultaneously flushing which displaces the air in the vial with the gas sample (Bretz and others 2021). Ambient air samples were taken to account for air CO_2 and CH4 concentrations when converting equilibrated headspace concentrations to wetland water concentrations. All samples, including air samples, were collected in triplicates. We analyzed headspace samples and ambient air samples for CO_2 and CH_4 on a gas chromatograph (Shimadzu Nexis GC-2030).

To assess parameters associated with CO_2 and CH_4 dynamics, we took samples for dissolved organic carbon (DOC), water isotopes ($\delta^{18}O$ and $\delta^{2}H$), nutrients, and ions. DOC samples were filtered through a 0.7-μM pre-ashed glass fiber filter (GFF) into acid washed and ashed amber glass vials in the field, kept on ice until acidified with HCl to a pH of ~ 2, and refrigerated at 4°C until analysis. DOC samples were analyzed within two weeks of collection by measuring non-purgeable organic carbon on a Shimadzu TOC-Vcph Carbon Analyzer. Water isotope samples were filtered with 0.45-μm polyethersulfone (PES) membrane filters into clear, glass vials in the field and stored at room temperature until analysis on a Picarro L1102-i Isotopic Liquid Water and Water Vapor Analyzer. Triplicate nutrient samples (total dissolved nitrogen [TDN], total dissolved phosphorus [TDP], and ammonium [NH_4^+]) and ions (chloride [Cl^-], sulfate [SO_4^{2-}], and nitrate [NO_3^-]) were filtered through 0.45-μm PES filters into 60-ml acid-washed HDPE bottles in the field, kept on ice in the field, and then frozen at -20°C until analysis. TDN, TDP, NO_3^-, and NH_4^+ were analyzed on a SEAL AutoAnalyzer 3 within two months of collection. Chloride (Cl^-) and sulfate (SO_4^{2-}) were analyzed on a Dionex ICS-3000. Sodium (Na^+), dissolved iron (Fe), and dissolved manganese (Mn) were analyzed on a Thermo iCAP RQ inductively coupled plasma with mass spectrometer (ICP-MS).

Dissolved Greenhouse Gas Calculations

Water CO_2 and CH_4 concentrations (GHG, μM) were estimated from GC peak areas using Henry's law, the ideal gas law, and the ratio of headspace to water in syringes. We estimated the partial pressure of CO_2 and CH_4 (pCO_2 and pCH_4, μatm) from the headspace samples as follows:

$$pGHG = \frac{pGHG_{samp} * KH_{lab} + \left(hsRatio * \frac{pGHG_{samp} - pGHG_{hs}}{molV}\right)}{KH_{site}} \quad (1)$$

$pGHG_{samp}$ (ppmv) is the concentration of CO_2 or CH_4 in the equilibrated headspace, *hsRatio* is the equilibration headspace ratio of water volume to gas volume (in this case, equal to 20 mL/20 mL or 1), $pGHG_{hs}$ (ppmv) is the concentration of CO_2 or CH_4 in the air used to equilibrate the samples, and *molV* (L mol^{-1}) is the molar volume based on temperature (K) and pressure (atm). *KH* (mol L^{-1} atm^{-1}) is the solubility constant for each respective gas, which is a function of temperature (in Kelvin) in the laboratory ($KH_{lab;}$ 20°C) and in the water during sampling (KH_{site}). Gas-specific KH formulas are in the supplement (*gas solubility constants*). Partial pressures of CO_2 and CH_4 (*pGHG*,

Table 3. Mixed-Effects Model Results for Surface Water CO_2

Null model: $[CO_2] \sim pH + [DO] + [CH_4] + SpC + Temperature + [DOC] + \delta^{18}O + log[TDP] + log[SO_4^{2-}] + [NO_3^-] + [NH_4^+] + [Fe] + [Mn] + daily\ mean\ water\ level$

Best Model: $[CO_2] \sim pH + [DO] + [CH_4] + Temperature + daily\ mean\ water\ level$

	Value	Std. error	DF	t-value	p-value
Intercept	866.3741	98.47161	47	8.798212	0
pH	− 33.4024	9.28917	47	− 3.59584	0.0008
[DO]	− 24.8112	6.94811	47	− 3.57092	0.0008
$[CH_4]$	3.3166	0.94327	47	3.516098	0.001
Temp (C)	− 11.2277	2.88254	47	− 3.89506	0.0003
Daily mean water level	− 146.254	68.21951	47	− 2.14387	0.0372

Summary of the best mixed-effects model for wetland CO_2 surface water concentrations, using site as a random effect. The values, standard errors, degrees of freedom (DF), t-values, and p-values are given for the intercept and for each fixed effect. The null model includes pH, dissolved oxygen (DO) concentrations, specific conductivity (SpC), temperature, dissolved organic carbon (DOC) concentrations, the water isotope $\delta^{18}O$, total dissolved nitrogen (TDN), total dissolved phosphorus (TDP), sulfate (SO_4^{2-}), nitrate (NO_3), ammonium (NH_4), iron (Fe), manganese (Mn), and daily mean water level. DO%, δ^2H, and total dissolved nitrogen (TDN) were removed because of being highly correlated (variance inflation factor > 5%) with DO concentration, $\delta^{18}O$, and NO_3, respectively.

μatm) were then converted to concentrations (*GHG*, μM), using the gas constant, *R* (0.08205601 L atm K^{-1} mol^{-1}), and temperature (T, K):

$$GHG = \frac{\left(pGHG\left(\frac{1}{R}\right)\left(\frac{1}{10^{-3}}\right)\left(\frac{1}{T}\right)\right)}{1000} \quad (2)$$

Statistical Analyses

All statistical analyses were conducted in R (version 5134.0.2; R Core Team 2020) and all figures were made using the ggplot2 package (Wickham 2016). We performed a Shapiro–Wilk test to evaluate normality using the *shapiro.test()*. Non-normal variables were log10-transformed before any statistical analyses.

We used coefficients of variation (CVs) to evaluate CO_2, CH_4, and hydrologic changes across time and among sites. Both temporal and site CVs were calculated, where temporal CVs reflect the variation in one site across all the sampling dates (n = 20) and site CVs reflect the variation across all sites within one sampling date (n = 11).

To evaluate differences in CO_2 and CH_4 across sites and water sources (surface water or groundwater), we used analysis of variance (ANOVA) with post hoc Tukey's honestly significant difference (HSD) tests. The ANOVA was performed using *aov()*, and the Tukey HSD was performed using *TukeyHSD()* in base R (R Core Team 2020).

Further analyses of correlated variables and modeling focuses solely on surface water dynamics. To analyze the relationships between surface water CO_2 and CH_4 concentrations and their respective CVs with water chemistry and other wetland characteristics, we performed linear regressions using the *lm()* function (R Core Team 2020). For each relationship, we accounted for multiple comparisons by correcting the *p*-values with a Bonferroni correction using the function *p.adjust()*. We also performed linear mixed-effects models for surface water CO_2 and CH_4 concentrations using the function *lme()* from the nlme package (Pinheiro and others 2021). The mixed-effects model was defined with site as a random intercept and a fixed slope. The null model included surface water CO_2 or CH_4 (for CH_4 or CO_2, respectively), nutrients (TDN and TDP), DOC, redox-sensitive ions (NO_3^-, SO_4^{2-}, Fe, and Mn), water isotopes ($\delta^{18}O$ and δ^2H), physicochemical variables (DO, specific conductance, temperature, and pH), and daily mean water level as fixed effects (full null model in Tables 3 and 4). Within *lme()*, we accounted for temporal autocorrelation (sample date) using a continuous-time

Table 4. Mixed-Effects Model Results for Surface Water CH_4

Null model: $[CH_4] \sim pH + [DO] + [CO_2] + SpC + Temperature + [DOC] + \delta^{18}O + log[TDP] + log[SO_4^{2-}] + [NO_3^-] + [NH_4^+] + [Fe] + [Mn] + daily\ mean\ water\ level$

Best model: $[CH_4] \sim pH + [CO_2] + [DOC] + [NH_4^+]$

	Value	Std. Error	DF	t-value	p-value
(Intercept)	− 19.8124	5.27663	− 60	3.75474	0.0004
pH	2.209479	0.583176	60	3.788703	0.0004
$[CO_2]$	0.030504	0.008185	60	3.727054	0.0004
[DOC]	0.183807	0.074615	60	2.463408	0.0166
$[NH_4^+]$	15.91305	2.877289	60	5.530571	0

Summary of the best mixed-effects model for CH_4 surface water concentrations, using site as a random effect. The values, standard errors, degrees of freedom, t-values, and p-values are given for the intercept and for each fixed effect. The null model includes pH, dissolved oxygen (DO), specific conductivity (SpC), temperature, dissolved organic carbon (DOC) concentration, the water isotope $\delta^{18}O$, total dissolved nitrogen (TDN), total dissolved phosphorus (TDP), sulfate (SO_4^{2-}), nitrate (NO_3), ammonium (NH_4), iron (Fe), manganese (Mn) and daily mean water level. DO%, δ^2H, and total dissolved nitrogen (TDN) were removed because of being highly correlated (variance inflation factor > 5%) with DO concentration, $\delta^{18}O$, and NO3, respectively.

first-order autoregressive model by defining *correlation = corCAR1()*. The null and final models were evaluated for multicollinearity using *check_collinearity()* from the performance package (Lüdecke and others 2021). Highly correlated variables (variance inflation factor > 5%) were removed and the *summary()* function was used to identify significant variables in the model (R Core Team 2020). We did final model checks of normality of residuals and multicollinearity using *check_model()* and evaluated predicted values against actual values using the *lm()* function (Figure S7).

Results

Variability in Surface Water and Groundwater CO_2 and CH_4 Concentrations

We found that groundwater had distinct CO_2 and CH_4 signatures from surface water. CO_2 concentrations were higher in groundwater (mean ± standard deviation = 1045.0 ± 590.0 µM) than in surface water (341.1 ± 162.8 µM) across all sites and dates ($p < 0.001$; Figure 2a). CH_4 concentrations, while highly variable in both surface water and groundwater, were higher in surface water (12.2 ± 17.7 µM) than in groundwater (6.1 ± 12.7 µM) and were significantly different ($p = 0.002$; Figure 2b). CO_2 and CH_4 were positively correlated (Figure 2c), with a stronger relationship in groundwater ($R^2 = 0.40$, $p < 0.001$) than in surface water ($R^2 = 0.20$, $p < 0.001$).

Surface water CH_4 was more dynamic than CO_2 over both space and time, and variability over space was larger than variability over time for both gases (Figure 3a,c). Temporal CVs, which indicate the variability over sampling dates for each wetland site, ranged from 17 to 200% with an average of 62% for surface water CO_2 and 74–176% with an average of 98% for surface water CH_4 (Figure 3a). And with the exception of 3 wetlands, temporal variability was always higher for CH_4 than for CO_2 (Figure 3a, points above the 1:1 line). Similarly, surface water CH_4 was more spatially variable than CO_2, with across-site CV averages of 100% and 60% when values from each sampling date were compared among sites, for CH_4 and CO_2, respectively (Figure 3c). Further, the variability in surface water CO_2 and CH_4 was, on average, larger among wetlands during a single sampling period (across-site CV) than over time at a single wetland (temporal CV). Interestingly, the temporal variability of CO_2 and CH_4 was not correlated with water level variability (Figure S1).

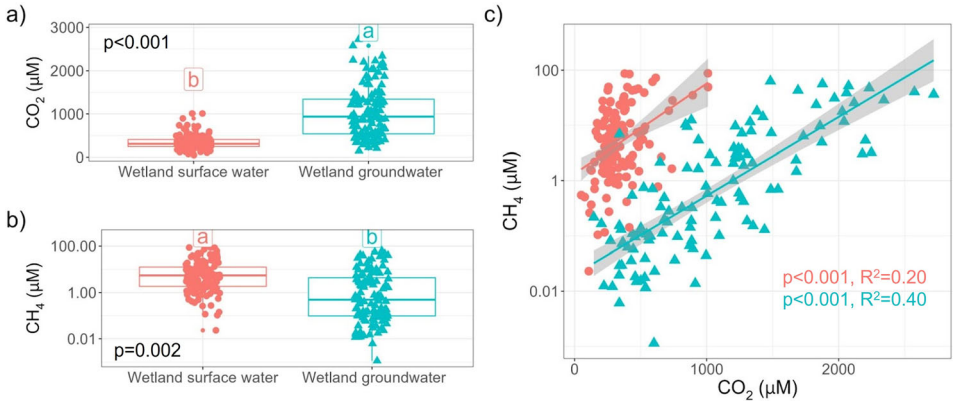

Figure 2. Concentrations of dissolved CO_2 (**a**) and CH_4 (**b**) in wetland surface water (pink circles) and groundwater (blue triangles) across 11 sampling dates and 20 wetlands. Horizontal lines in the boxplots represent the surface water and groundwater CO_2 and CH_4 medians; lower and upper box boundaries are the 25th and 75th percentile, respectively. Vertical lines are the 95% confidence interval. Letters above each boxplot note a significant difference between surface and groundwater based on a Tukey honest significant difference test ($p < 0.05$). **c** There was a significant positive relationship between CH_4 and CO_2 in both surface water (pink circles) and groundwater (blue triangles) (**c**). Linear regression lines, shading which represents the 95% confidence interval, and corresponding linear model statistics are shown. Note that the CH_4 axis is log-transformed.

In groundwater, similar patterns hold and CH_4 was much more variable than CO_2 with all sites and sampling dates falling above the 1:1 line (Figure 3b, d). Over time, the CO_2 temporal CV averaged 33% (13–64%) and the CH_4 CV averaged 136% (45–280%). Spatially, the CH_4 CV average was 195% (112–297%) and the CO_2 CV average was 55% (33–69%). In contrast to surface water, groundwater CH_4 was more temporally and spatially variable, while CO_2 was less variable and more constrained (note difference between the axes in Figure 3).

Wetland Hydrogeomorphic Characterization

Wetland maximum flooded area (hereafter, ''wetland area'') ranged from 379 m^2 to 6410 m^2, with an average of 1431 m^2 (Table 1, Figure 1h). Wetland area correlated strongly with wetland maximum flooded volume (hereafter, ''wetland volume''), and therefore only wetland area was used for subsequent analyses ($p < 0.001$, $R^2 = 0.93$; Figure S2a). Perimeter:area ratios also have a nonlinear, negative relationship with area, with some wetlands diverging from a linear relationship indicating a more complex morphology ($p < 0.01$, $R^2 = 0.58$; Figure S2b). Wetland elevation is similar across the 20 wetland sites used in this study, ranging from 14.8 m to 19.2 m ASL (Table 1).

Surface Water Greenhouse Gas and Water Chemistry Patterns Across Sites

Across the landscape, surface water CO_2 and CH_4 concentrations were variable, with wetland averages across all sampling events ranging from 123.7 to 605.0 µM for CO_2 and from 1.7 to 46.1 µM for CH_4 (Table 2, Figure 4). Some wetlands had higher temporal variability, while others had more constrained ranges, though it is worth noting that some wetlands were sampled more times than others, given hydrologic conditions during each sampling period (Figure S3a). CO_2 and CH_4 were significantly different among wetlands ($p < 0.001$). There were 3 groups of wetlands with significantly different mean concentrations for CO_2 and 4 groups for CH_4 (Figure 4). We also found that F1 had significantly higher CO_2 and CH_4 concentrations than all other wetlands ($p < 0.001$). While not the focus of our study, three out of four emergent vegetation wetlands (those denoted with the letter E) had the lowest concentrations of CO_2, while all four in the study had the lowest concentrations of CH_4 (Figure 4). Sites within wetland complexes were not statistically different with respect to CO_2 ($p = 0.45$; Figure 4, Figure S4a) or CH_4 ($p = 0.42$; Figure 4, Figure S4b) concentrations.

Water chemistry also varied widely across sites (Table 2). Average wetland pH ranged from 3.9 to 7.4, with generally acidic conditions across the wetlands. Some wetlands had particularly high specific conductivity such as wetland F11 with a

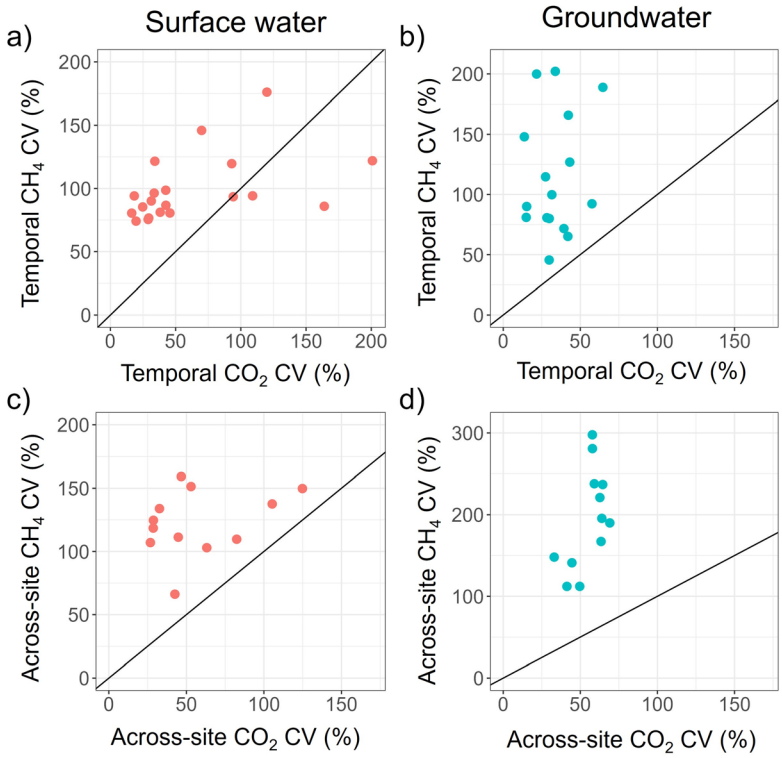

Figure 3. Temporal coefficients of variation (CV) for CH_4 and CO_2 in surface water (**a**) and groundwater (**b**) for each headwater wetland (n = 20) represent the temporal variability over the whole study period for each wetland. Across-site CVs for CH_4 and CO_2 in surface water (**c**) and groundwater (**d**) represent the variability across all the wetlands for each sampling date (n = 11). Each point in the top panel represents a wetland, while each point in the bottom panel represents a sampling date. Note the difference in axes scales for across-site CH_4 CVs (**c**, **d**).

mean of 113.1 uS/cm, but generally wetlands ranged from 20.1 to 69.5 uS/cm. Wetlands in our study were also low in DO with most sites below 6 mg/L with only 7 wetlands averaging between 6.1 and 8.7 mg/L. Nutrients were generally low, with the highest average TDN of 2.8 mg/L. Average DOC concentrations were high across sites with a lowest site mean of 21.4 and a highest of 55.9 mg/L.

Average wetland surface water CO_2 was not correlated with maximum inundation area (p = 1.0; Figure 5a), but smaller wetlands had variable and generally higher CH_4 concentrations, though very weakly correlated ($p < 0.005$, R^2 = 0.07; Figure 5d). Wetlands with higher perimeter:area and HAND values had higher average surface water CO_2 and CH_4 concentrations. Perimeter:area, which indicates increasing morphological complexity and aquatic-terrestrial interfaces with higher values, was significantly positively correlated with CO_2 ($p < 0.001$, R^2 = 0.23; Figure 5b) and CH_4 ($p < 0.001$; R^2 = 0.11; Figure 5e), though the relationship with CO_2 was stronger. HAND, a proxy of closeness to the larger fluvial network, was weakly positively correlated with average CO_2 concentrations but with a very low explanatory power ($p < 0.05$, R^2 = 0.04; Figure 5c) and was more strongly correlated with CH_4 concentrations ($p < 0.001$; R^2 = 0.23; Figure 5f).

Hydrologic and Surface Water Greenhouse Gas Temporal Dynamics

Over time, all wetlands were hydrologically variable, with wetland water levels across all sites ranging from − 0.7 m (water level below 0 indicates a period in which the wetland went dry) to 1.1 m (Figure S3a). Water levels throughout our sampling period tracked expected seasonal patterns. In all wetlands, the water level was relatively stable during early spring but decreased during the summer months of 2021. This was followed by a wet-up event and an increase in water level in September 2021. Water level decreased slightly after the fall wet-up and continued experiencing short wet-up events, ultimately stabilizing in winter and early 2022. The 2022 dry-down began in late fall and into the summer, a period in which most of our wetlands completely dried out. Smaller

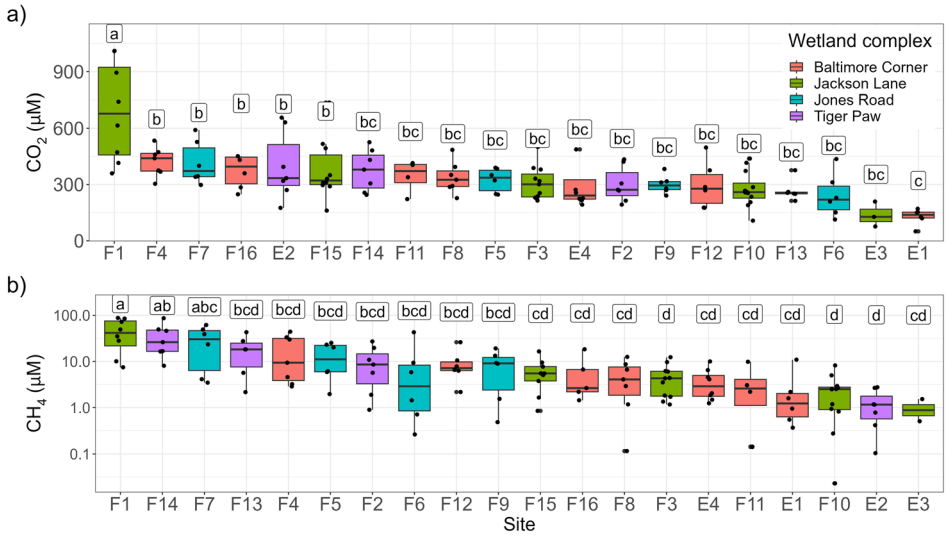

Figure 4. Boxplots of concentrations of surface water dissolved CO_2 (**a**) and CH_4 (**b**) across all wetlands (n = 20), colored by their corresponding wetland complex. Horizontal lines in the boxplots represent the site median; lower and upper box boundaries are the 25th and 75th percentile, respectively. Vertical lines are the 95% confidence interval. Note that the y-axis in (**b**) is log10-transformed. Data in this figure represent samples taken every 2–3 months over the course of 2 years, where each point within a box is a different sampling date. The number of points within each site varied depending on how many times each wetland was sampled and is not consistent across sites. Sites are arranged in order of highest to lowest average concentration and significant differences across sites are denoted with different letters (Tukey's honest significant difference, $p < 0.05$).

wetlands dried earlier and also experienced higher hydrologic variability (Figure S5).

Seasonal and longer-term water level changes also potentially resulted in changing redox and greenhouse gas dynamics over the 2-year time period (Figure S3). Dissolved oxygen (DO) ranged from 2.9 to 7.5 mg/L and the lowest average concentrations of 1.4 mg/L occurred during the summer period of 2021 with consequent slow increases in DO (Figure S3b). The highest concentrations in DO occurred at the end of our study period between fall (range = 5.42–9.65 mg/L) and winter (range = 3.27–10.77 mg/L) of 2022. CO_2 variability across sites was low during stable hydrologic moments and was more responsive to the wet-up events than to drying down (Figures 3c, S6b). The period preceding our study had relatively stable hydrologic conditions, and during the late spring and summer dry-down period of 2021, surface water CO_2 concentrations began increasing. CO_2 concentrations peaked during fall and winter after the dry-down period in which almost half of the wetlands in our study went dry (Figure S3a, c). Into spring 2022 when water level stabilized, CO_2 concentrations decreased. This period was followed by a rapid drying period in summer, in which all but one of our wetlands dried out, leading to fewer sampling periods. Following a late fall wet-up after a long dry period, CO_2 concentrations were more variable but stabilized by winter. CH_4 decreased consistently from December 2020 to December 2022, and average concentrations had little response to key hydrologic moments or seasons, with the exception of a slight increase in CH_4 following the summer 2021 wet-up (Figure S3d). Interestingly, CH_4 variability among wetlands was also lower during stable hydrologic periods and seemed to change more during dry down than during wet-up periods (Figure S6b).

Daily mean water level correlated with CO_2 in surface water and did not correlate with CH_4 in surface water (Figure 6). We observed higher CO_2 concentrations with lower daily mean water level across the wetlands ($p < 0.001$, $R^2 = 0.11$; Figure 6b). However, we did not observe a relationship between CH_4 and daily mean water level ($p = 0.9$, $R^2 = 0.01$) and higher CH_4 concentrations occurred across the range of different water levels.

Mixed-Effects Models

Mixed-effects models of surface water CO_2 and CH_4 indicated that a combination of biogeochemical conditions influences carbon dynamics in these wetlands, and that some influences on CO_2 and CH_4 are site-specific. In our mixed-effects models, we included water level, all water chemistry parameters (DOC, anions, cations, and water iso-

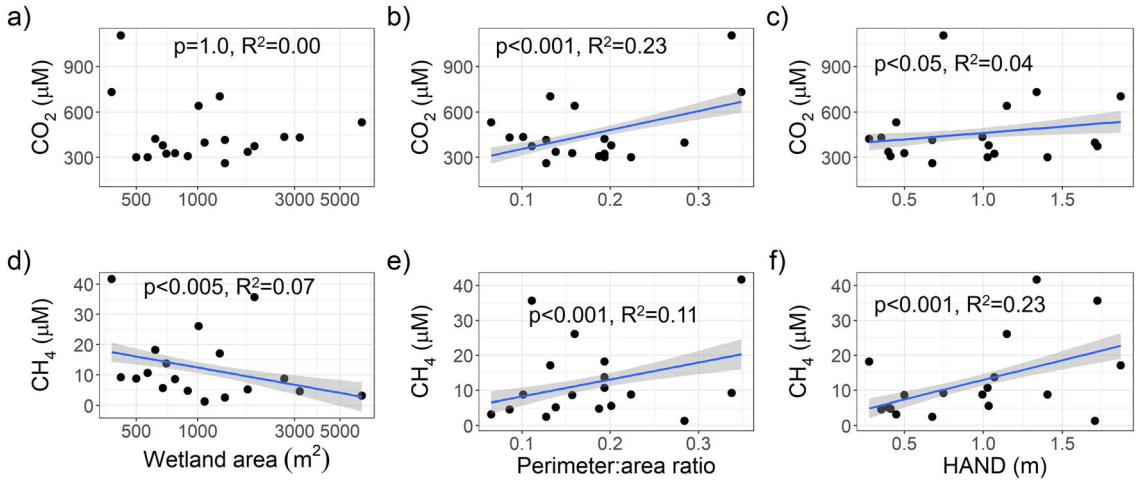

Figure 5. Relationships of average CO_2 and CH_4 concentrations with different wetland morphological variables across 18 of our wetland sites and their corresponding statistics. **a–c** CO_2 concentrations and **d–f** CH4 concentrations with wetland area (**a**, **d**), perimeter:area ratio (**b**, **e**), and height above drainage network (**c**, **f**). Lines are the best-fit linear model for each relationship and shading around the lines is the standard error. Panels with statistics but no lines represent non-significant linear relationships ($p > 0.05$).

topes) as well as water physicochemical parameters (DO, specific conductance, temperature, and pH) as potential drivers of CO_2 and CH_4. We also included CH_4 as a potential driver of CO_2 and CO_2 as a potential driver of CH_4.

Significant fixed effects for surface water CO_2 were pH ($p = 0.0008$), DO concentrations ($p = 0.0008$), CH_4 ($p < 0.001$), temperature ($p = 0.0003$), and daily mean water level ($p = 0.03$), and the overall model was statistically significant (F = 396.8, $p < 0.0001$, $R^2 = 0.6$; Table 3). In the CO_2 model, 56% of the variance was attributed to a site effect. The overall CH_4 model was also statistically significant (F = 52.5, $p < 0.0001$, $R^2 = 0.6$; Table 4), with significant fixed effects: pH ($p = 0.004$), CO_2 ($p = 0.004$), NH_4^+ ($p = 0.00$), and DOC ($p = 0.01$). The CH_4 model had a lower influence of site, with only 28% of the variance attributed to the site effect. To specifically evaluate why DO was not a significant predictor in the CH_4 surface water model and to compare with the CO_2 model, we also performed linear regressions and found that CO_2 concentrations were higher under lower oxygen conditions and that CH_4 concentrations were generally higher but variable below 6 mg/L and constrained above this threshold (Figure S7). Predicted values of CO_2 ($R^2 = 0.74$) and CH_4 concentrations ($R^2 = 0.69$) against actual concentration show a good performance of both models with a better performance of the CO_2 model (Figure S8). Residuals for the CO_2 model ranged from − 181.2 to 214.60 and for the CH_4 model from − 26.1 to 29.9.

Discussion

This study quantified and evaluated the controls on concentrations and variability in headwater wetland CO_2 and CH_4 across a hydrologically dynamic wetland landscape. We found that wetlands with higher perimeter:area had higher concentrations of CO_2 and CH_4 and that the temporal variability was driven by a combination of changing hydrology and biogeochemical controls. Our results suggest that CH_4 was governed by the high availability of substrate and associated redox conditions, while CO_2 concentrations were associated with high-concentration groundwater inputs and hydrologic changes. At the landscape scale, we found that wetland hydrogeomorphic characteristics explained general patterns in CO_2 and CH_4: smaller wetlands and, in particular, wetlands with a higher perimeter:area ratio had higher average CO_2 and CH_4 concentrations, and wetlands higher in the landscape with higher HAND values had higher average CH_4 concentrations. Further, CH_4 was much more variable than CO_2, and the variability in surface water CO_2 and CH_4 concentrations across sites was larger than the variability over time.

Different Sources and Mechanisms Sustain CO_2 and CH_4 Supersaturation

The relationships between wetland CO_2 and hydrology, based on the pattern of higher CO_2 concentrations with lower water level (Figure 6), suggest that CO_2 is sustained by inputs of CO_2-enriched groundwater (Figure 2). Groundwater

tends to have higher concentrations of CO_2 due to the accumulation of soil and root respiration (Nikolenko and others 2019) and even varies among wetlands dominated by different plants (Sharp and others 2024). In the soils surrounding wetlands, CO_2 can accumulate in the soil environment and later be transported to the wetland (Limpert and others 2020). Sustained groundwater inputs can provide a stable source of CO_2 or CO_2 accumulated in the subsurface could be flushed into the wetland during rain events. The role of groundwater as a source of surface water CO_2 has been extensively documented, particularly in headwater streams (Hotchkiss and others 2015; Duvert and others 2018; Lupon and others 2019) and coastal wetlands (Wang and others 2022) but less so in freshwater inland wetlands. Our sampling approach was not fine enough to capture daily or weekly responses to rain events and changing groundwater contributions but rather was able to capture seasonal changes in groundwater, with groundwater potentially having a higher contribution to wetland CO_2 during fall and winter when evapotranspiration is not as high as in the late spring and summer. Seasonally, once the wetlands dry out, oxygen becomes more available and decomposition happens more rapidly, producing CO_2 (Altor and Mitsch 2008). We observed increases in CO_2 during and after a wet-up period which highlights that the changing hydrologic conditions that influence oxygen availability have the potential to change decomposition rates (Figure S5). Further, changing hydrologic conditions shift groundwater contributions and rain events flush CO_2 into the wetlands (Webb and others 2016).

Other processes, such as aerobic respiration and the production of CO_2 through CH_4 oxidation, could also be contributing to sustaining CO_2 sources in these wetlands. The negative relationship between CO_2 and DO (Figure S7a) as well as the positive relationship between CO_2 and CH_4 seen in the mixed-effects models (Table 4) potentially indicates production of CO_2 from the oxidation of CH_4, particularly produced in the more oxygenated groundwater (Zhu and others 2023). Similarly, dissolved organic matter (DOM) released from mineral subsurface soils that are frequently hydrologically connected to groundwater in this landscape has a microbial-like signature, which in turn can provide a reactive organic matter source to wetlands (Wardinski and others 2022). For example, the delivery and subsequent mineralization of soil-derived DOM can increase CO2 production in wetlands (Rasilo and others 2017). However, dissolved organic carbon (DOC) was not a significant

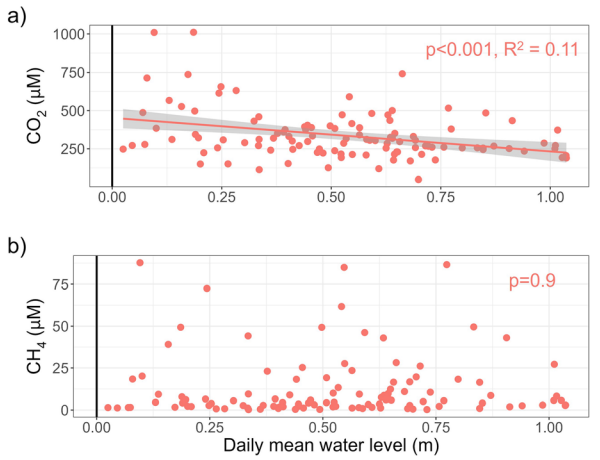

Figure 6. Relationships of surface water CO_2 (**a**) and CH_4 (**b**) concentrations with daily mean wetland water level. Black vertical line indicates the ground surface. Linear regressions are shown for the significant relationships with corresponding statistics. The relationship between CH_4 and daily mean water level was not significant.

effect in the CO_2 mixed-effects model, suggesting that the availability of substrate for mineralization was not limiting CO_2 production. Ultimately, changing water level as well as seasonal changes in groundwater contributions to surface water might be more important in controlling CO_2 concentrations in these wetlands.

CH_4 supersaturation in headwater wetlands is likely sustained by production in anoxic sediments, influenced by water column biogeochemical conditions, and possibly altered by stratification in larger and deeper wetlands. Compared to CO_2 dynamics, we saw little influence of water level variation on CH_4 (Figure 6, S3). Since CH_4 production is less energetically favorable and CH_4 can be quickly oxidized in higher DO unsaturated zones, groundwater is unlikely to be a direct source of CH_4 to our study wetlands. This stands in contrast with the stream biogeochemistry literature, which has reported that both CO_2 and CH_4 can be sourced from groundwater (Lupon and others 2019). Instead, it is more likely that CH_4 is produced in the anoxic wetland sediments. Given that our wetlands are relatively shallow and low in DO (Tables 2 and 3), there are fewer opportunities for CH_4 oxidation to occur as CH_4 moves into the water column prior to being emitted from the wetland surface. Further, the relationship observed in the mixed-effects models between CH_4 and CO_2 could suggest that CH_4 production from CO_2 through the hydrogenotrophic methanogenesis pathway might also be occurring in the less oxy-

genated surface waters (Zhu and others 2023). We also found higher CH_4 concentrations with increased dissolved organic carbon (DOC) in surface water (Table 4). Additions and inputs of organic matter can also stimulate CH_4 production, and given the high concentrations of DOC in these wetlands and its low oxygen conditions, the production of CH_4 can be large (Grasset and others 2018). Similar to studies evaluating the role of inundation on CH_4 dynamics in the same region (Hondula and others 2021b), we found that the magnitude of water level did not explain changes in CH_4. However, this previous work also found that the direction of water level was important, with decreasing water levels showing higher CH_4 emissions. Over a longer timescale of two years, we observed decreasing CH_4 and increasing DO, which could indicate that Delmarva headwater wetlands are becoming more aerobic due to consistent drying patterns within our study period. This drying can lead to lower CH_4 production and/or increased CH_4 consumption and consequently, decreases in CH_4 concentrations.

Temporal variability across wetlands was driven by a combination of water level and corresponding biogeochemical and physicochemical conditions. For surface water CO_2 concentrations, pH, DO, CH_4, temperature, and daily mean water level were significant drivers in the mixed-effects model, with higher CO_2 concentrations associated with lower DO, higher CH_4, lower water temperature, and lower water level (Table 3)—all related to hydrologic controls on CO_2, as previously discussed. In addition, our results highlight the strong site specificity, with a site effect of 54% in the CO_2 model, potentially driven by the influence of size and area:perimeter. Surprisingly, the relationship of CO_2 with temperature was negative, contrasting the predicted pattern that respiration would increase with increasing temperature (Yvon-Durocher and others 2014). The complex interaction among the many factors that influence gas dynamics or changing availability of reactive organic matter substrates may be masking the temperature effects. For example, in these shallow wetlands, it is possible that the relationship with temperature is modulated by water level (Chen and others 2021).

In the CH_4 model, we found significant effects of pH, CO_2, DOC, and NH_4^+ with higher DOC, NH_4^+, CO2, and pH corresponding to higher CH_4 concentrations (Table 4). In contrast, the site effect for CH4 was 20%, which was lower than the site effect of the CO_2 model. The combination of DOC and NH_4^+ driving CH4 underscores the importance of substrate availability and highlights how CH_4 production could increase with increasing nutrient concentrations. Increased NH_4^+ likely suppresses CH_4 oxidation and enhances CH_4 production, therefore leading to increased CH_4 emissions (Liu and Greaver 2009), which has important implications as we consider the impact of increasing nutrient concentrations in freshwater ecosystems globally. Interestingly, dissolved DO was not a significant effect in the CH_4 model. This is possibly due to the nonlinearity of the relationship of CH_4 with DO (Figure S7), in which CH_4 concentrations are higher and more variable below $\sim$ 4 mg/L DO and remain relatively constrained (less than 25 μM) above that DO threshold. Under low oxygen conditions, terminal electron acceptors have been used and the reduction of CO_2 and fermentation of acetate to produce CH_4 are favored. Whether CO_2 or acetate is used to produce CH_4 depends on the availability of the substrates and the dominant methanogenic communities and more specific isotopic or microbial work is needed to elucidate the actual pathways of this CH_4 production.

CH_4 as More Dynamic Over Time and Across the Landscape than CO_2

In addition to high concentrations of CO_2 and CH_4, CO_2 and CH_4 variability over space and time was substantial. We found that CH_4 was generally more variable (both over space and time) than CO_2, and that this variability was slightly higher than what has been reported in other studies for both wetland CO_2 and CH_4 (Holgerson and Raymond 2016; Hondula and others 2021b). For example, globally, Holgerson and Raymond (2016) looked at small lakes and ponds and quantified an average CO_2 concentration of 133.99 μM with a 16.69 μM standard error and a CH_4 concentration average of 7.57 μM with a standard error of 1.64 μM for size classes below 0.001km^2, which are comparable to our study sites (range = 0.00038–0.00641 km^2, Table 2). In contrast, our study average for CO_2 was 365.4 μM with a standard error of 20.1 μM and for CH_4, a mean of 11.8 μM with a standard error of 2.3 μM. Further, our observed CH_4 variability over time is potentially underestimated given that our sampling did not capture ebullition, which is a substantial and highly variable flux of CH_4 given CH_4's low solubility in water (Crawford and others 2014). The lower temporal variability of CO_2 in contrast to CH_4 could be due to the sustained and relatively stable groundwater CO_2 contribution. On the other hand, production pathways and sources

for CH_4 might be influenced by a larger combination of environmental factors and therefore more dynamic and complex (Bridgham and others 2013). Aerobic CH_4 production could result in different CH_4 production rates across different hydrologic conditions and redox conditions (Wang and others 2022; Mao and others 2024), but the availability of reactive organic matter may limit when and where oxic CH_4 production can occur in wetlands. Importantly, our results that show the different controls on CH_4 and CO_2 highlight the increased need to resolve spatiotemporal variability, particularly for CH_4.

Spatial variability is also higher than temporal variability showing that within-seasonal patterns are constrained relative to differences across sites (Figure 3). Higher spatial variability of CO_2 and CH_4 in our study points to a large landscape heterogeneity, which could increase during periods of hydrologic disconnection (Figure S6). Soil carbon stocks at these same sites are also highly variable (Stewart and others 2023). On a relatively small landscape scale, we also found that CO_2 and CH_4 patterns in the wetlands were not associated with wetland complex (Figures 4, S4). We expected some spatial patterns driven by wetland complexes due to more localized precipitation events and watershed soil conditions, which we did not observe. In addition, wetlands within wetland complexes can experience surface water connections, potentially mixing water sources and making greenhouse gas dynamics more homogenous within wetlands close to each other. However, we did not observe homogenization of CO_2 or CH_4 and instead found large effects of site-specific relationships, particularly for CO_2, which are discussed in more detail below. Small-scale processes, such as landscape heterogeneity due to anoxic microsites and particular microbial communities or biological interactions, could then be driving the high spatial variability (Koch and others 2014). Broader regional controls like hydrogeomorphology and regional climate patterns, which are beyond the scale of this work, might also drive greenhouse gas concentrations patterns (Hassan and others 2023). While not a specific objective of this work, we also found that emergent vegetation wetlands generally had lower CH_4 and CO_2 concentrations. The role of vegetation in greenhouse gas emissions can be substantial (Jeffrey and others 2019). Our findings highlight the need for increased bottom-up measurements of greenhouse gas concentrations and emissions across different types of wetlands given the difficulty in generalizing patterns at the subcatchment scale.

Wetland Hydrogeomorphology Influences Greenhouse Gas Dynamics

In comparison with other studies focused on small, freshwater wetlands, our wetlands were generally smaller ($< 7{,}000 m^2$, Figure 1), which fills a knowledge gap of CO_2 and CH_4 concentrations in small and hydrologically variable wetlands, ecosystems missing from many pond and wetland studies. Smaller, more morphologically complex (that is, higher perimeter:area) wetlands have higher dissolved CO_2 and CH_4 surface water concentrations. We did not see a relationship with wetland area and CO_2, but we did see a negative relationship, though very weak, with wetland area and CH_4 (Figure 5). However, the low R^2 of 0.07 for the relationship between area and CH_4 highlights that there remains a lot of variability that is not explained solely by area. We did see a positive relationship of both CO_2 and CH_4 with perimeter:area, indicating the importance of the shape and terrestrial-aquatic interfaces of the wetland in driving the perimeter:area-GHG relationship, particularly for CO_2. In particular, these relationships with perimeter:area had higher explanatory power than the relationships with area, with an R^2 of 0.23 for CO_2 and 0.11 for CH_4. Higher concentrations of CO_2 in the smaller, more morphologically complex wetlands we monitored further suggest that groundwater inputs across the terrestrial-aquatic interface could be a substantial source of CO_2, particularly in ecosystems that are highly connected to their terrestrial environment and have greater perimeter:area for inputs. A higher perimeter:area indicates an increased reactive interface which implies increased interactions with the sediment, providing a larger area for CH_4 production as well as increased inputs of high-CO_2 groundwater from the terrestrial landscape (Downing 2010). Higher CO_2 concentrations in smaller wetlands have also been documented at the global scale (Holgerson and Raymond 2016) as well as in other more localized studies in the Arctic (Ludwig and others 2022) as well as Canada and Chile (Hassan and others 2023). Smaller wetlands tend to be more sheltered from wind shear and have lower reaeration coefficients which can prevent gas exchange to the atmosphere (Richardson and others 2022). Given that reaeration can affect both CO_2 and CH_4, we would have also expected to see a negative relationship between wetland area and CO_2, which is similarly influenced by gas exchange, but we did not. Therefore, other variables besides gas exchange play a part in the observed CO_2 and CH_4 relationship with area. Small wet-

lands also have high connectivity to the landscape which can provide direct inputs of organic matter substrates for CO_2 and CH_4 production (Holgerson 2015; Ludwig and others 2022; Richardson and others 2022).

Our results also highlight the landscape scale patterns that can emerge and point to the potential role of transport, gas exchange, and metabolic processes in modifying these patterns. We found that average wetland CH_4 concentrations and on a lesser scale, CO_2 concentrations, were higher in wetlands with higher HAND values (Figure 5). HAND can serve as a proxy height above the water table or the relative position along the hillslope transect. A low HAND value suggests the wetland is toward the bottom of the hillslope and, importantly, suggests it intersects more readily with the groundwater table (Savenije 2010). Inversely, a high value of HAND suggests the wetland is toward the top of the hillslope and thus likely has less access to the water table. HAND can serve as a proxy of the relative closeness to the nearest drainage outlet, with a higher HAND representing a higher network position (Rennó and others 2008). While the wetlands in the Delmarva landscape do not experience consistent surface water connections, any brief surface connection can represent a substantial movement of water and solutes (Lee and others 2023). In addition, the subsurface and groundwater are locally and regionally connected, with potential for transport down the network through subsurface flowpaths (McLaughlin and others 2014; Lane and others 2018). While turbulence is relatively low in these wetlands, both CO_2 and CH_4 are being outgassed as they move down the network and into larger wetlands, potentially decreasing surface water concentrations if the degassing flux is larger than inputs. Within each wetland complex, some wetlands are spatially arranged downstream from each other and experience intermittent surface connections. Thus, with lower HAND values, there is an increased opportunity for transport down the network and decreased average CO_2 and CH_4 concentrations (Figure 5). We expected within-network patterns to be particularly strong within the more connected wetlands versus wetlands that are truly isolated in the landscape. In theory, wetland order would therefore be a useful variable to evaluate how CO_2 and CH_4 might be outgassing; however, given our high representation of 1st-order wetlands, this evaluation is better suited to a spatially broader approach. Further, the positive relationship between CH_4 concentrations and HAND in our results could point to biological mechanisms. When CH_4 is produced, usually within the anoxic sediment, it can be oxidized as it moves into more oxic parts of the wetland landscape (Ward and others 2020). In this context, lower CH_4 concentration in sites closer to the outlet of a network (lower HAND) could point to the role of higher CH_4 oxidation rates that decrease CH_4 concentrations as CH_4 makes its way down the network.

Inundated Headwater Wetlands are Hotspots of CO_2 and CH_4

Regardless of location or time of year, small, headwater wetlands were always supersaturated in CO_2 and CH_4 with respect to the atmosphere during our study, highlighting their consistent role as CO_2 and CH_4 sources on the landscape (Figure 4). In years with less rainfall, wetlands in our study region can be CH_4 sinks when they are not inundated (Hondula and others 2021b). Other wetland ecosystems, particularly coastal wetlands, also can alternate between sinks and sources of carbon due to environmental conditions and changing inundation regimes. For example, wetlands with high gross primary production compared to ecosystem respiration can take up more CO_2 than they emit, and this can change seasonally with changing temperatures, water level, and light dynamics (Kominoski and others 2021). Similarly, there might be periods in which wetlands are negligible CH_4 sources or sinks due to increasing aerobic conditions which promote CH_4 oxidation and decrease CH_4 production (Gleason and others 2009). In cases in which wetlands are also acting as CO_2 or CH_4 sinks, their ultimate contribution to carbon emissions depends on the difference between uptake, burial, emissions, and hydrological transport of both CO_2 and CH_4. However, our study suggests that inundated portions of headwater wetlands on the Delmarva Peninsula are persistent sources of both gases, which contrasts with other wetland ecosystems that might shift between sources and sinks. It is possible this shift between source and sink could also occur within these wetlands and long-term monitoring will be an important component of further understanding these source-sink dynamics. CO_2 and CH_4 concentrations in this study are comparable to other small, isolated wetland estimates and fall within the higher ranges of broader global wetland concentrations (Badiou and others 2011; Kifner and others 2018; Hondula and others 2021b). The higher concentrations in these small, headwater ecosystems across regions and globally highlight the potential role of freshwater inland wetlands with high organic matter concen-

trations and high terrestrial connectivity to serve as biogeochemical hotspots of carbon emissions, with important implications for future management, particularly in the context of wetland restoration (Kolka and others 2018; Rosentreter and others 2021).

Conclusion

Our findings confirm the potentially disproportionate and dynamic role that small, headwater wetlands can play as biogeochemical hotspots of CO_2 and CH_4 emissions and export (Marton and others 2015; Cohen and others 2016; Hondula and others 2021b). Headwater wetlands are numerous in many landscapes and could ultimately contribute large amounts of carbon to the atmosphere, suggesting a critical need to incorporate the magnitude and variability of CO_2 and CH_4 in headwater wetlands into global carbon models and upscaling efforts. We also documented large spatial variability in CO_2 and CH_4 among wetlands associated with maximum inundation area, perimeter:area ratios, and height above the nearest drainage. Our findings support the growing understanding that CO_2 and CH_4 dynamics represent one of the more complex and variable carbon fluxes in wetlands, with differing controls on CO_2 and CH_4 driving differences on their spatial and temporal variability. While not assessed in this study, dry periods likely represent moments in which the wetlands are CO_2 and CH_4 sinks (Hondula and others 2021b) and future studies integrating dry and wet emission fluxes will further improve our understanding of the role of headwater wetlands in landscape carbon budgets. More broadly, future work developing multi-annual wetland carbon budgets to identify how CO_2 and CH_4 concentrations and fluxes compare to other wetland carbon fluxes, such as soil storage and net ecosystem production, is necessary to characterize the ultimate contribution of headwater wetlands to landscape and global carbon cycling on longer time scales. Finally, land use alterations and climate change-induced changes in hydrology and increasing temperatures can drastically alter wetland carbon dynamics (Peng and others 2022), while small wetlands have recently lost many of their federal protections in the USA, establishing them as highly vulnerable ecosystems (Lane and others 2023). Evaluating the impacts of disturbance and climate change on CO_2 and CH_4 production, consumption, transport, and emissions, both empirically and experimentally, will help us predict what these dynamics can look like in the future to better inform their conservation and management.

Acknowledgements

We appreciate the help of Bobbie Niederlehner and Kelly Peeler for help with sample analysis and for support with analytical methods. We would also like to acknowledge the Virginia Tech Statistical Application and Innovations group for their support with the development of the mixed-effects model. We also acknowledge the input, feedback, and support of many colleagues over the years, in particular, Hotchkiss laboratory members and Virginia Tech Stream Team members. Finally, we greatly appreciate and acknowledge The Nature Conservancy for access to the sites and their protection of this land. This project was funded by NSF DEB award #1856560 to DM, ERH, & DS and #1856200 to MP. Support for CLL was provided by the Society for Freshwater Science Endowment award, an NSF DGE award #1840995, and the William Walker Fellowship through the Virginia Water Resources Research Center.

Data Availability

Data for this publication and code for analysis are available through the Environmental Data Initiative (EDI) portal at https://doi.org/10.6073/pasta/e74f71a429fc6d9f8db15fb5debcabc5 (López Lloreda and others 2024).

REFERENCES

Abril G, Borges AV. 2019. Ideas and perspectives: Carbon leaks from flooded land: do we need to replumb the inland water active pipe? Biogeosciences 16:769–784.

Altor AE, Mitsch WJ. 2008. Methane and carbon dioxide dynamics in wetland mesocosms: Effects of hydrology and soils. Ecological Applications 18:1307–1320.

Angle JC, Morin TH, Solden LM, Narrowe AB, Smith GJ, Borton MA, Rey-Sanchez C, Daly RA, Mirfenderesgi G, Hoyt DW, Riley WJ, Miller CS, Bohrer G, Wrighton KC. 2017. Methanogenesis in oxygenated soils is a substantial fraction of wetland methane emissions. Nature Communications 8:1567.

Badiou P, McDougal R, Pennock D, Clark B. 2011. Greenhouse gas emissions and carbon sequestration potential in restored wetlands of the Canadian prairie pothole region. Wetlands Ecology and Management 19:237–256.

Bretz KA, Jackson AR, Rahman S, Monroe JM, Hotchkiss ER. 2021. Integrating ecosystem patch contributions to stream corridor carbon dioxide and methane fluxes. JGR Biogeosciences 126:e2021JG006313.

Bridgham SD, Megonigal JP, Keller JK, Bliss NB, Trettin C. 2006. The carbon balance of North American wetlands. Wetlands 26:889–916.

Bridgham SD, Cadillo-Quiroz H, Keller JK, Zhuang Q. 2013. Methane emissions from wetlands: biogeochemical, microbial, and modeling perspectives from local to global scales. Global Change Biology 19:1325–1346.

Chen H, Xu X, Fang C, Li B, Nie M. 2021. Differences in the temperature dependence of wetland CO_2 and CH_4 emissions vary with water table depth. Nature Climate Change 11:766–771.

Cohen MJ, Creed IF, Alexander L, Basu NB, Calhoun AJK, Craft C, D'Amico E, DeKeyser E, Fowler L, Golden HE, Jawitz JW, Kalla P, Kirkman LK, Lane CR, Lang M, Leibowitz SG, Lewis DB, Marton J, McLaughlin DL, Mushet DM, Raanan-Kiperwas H, Rains MC, Smith L, Walls SC. 2016. Do geographically isolated wetlands influence landscape functions? Proceedings of the National Academy of Sciences USA 113:1978–1986.

Cozannet M, Le Guellec S, Alain K. 2023. A variety of substrates for methanogenesis. Case Studies in Chemical and Environmental Engineering 8:100533.

Crawford JT, Stanley EH, Spawn SA, Finlay JC, Loken LC, Striegl RG. 2014. Ebullitive methane emissions from oxygenated wetland streams. Global Change Biology 20:3408–3422.

Creed IF, Lane CR, Serran JN, Alexander LC, Basu NB, Calhoun AJK, Christensen JR, Cohen MJ, Craft C, D'Amico E, DeKeyser E, Fowler L, Golden HE, Jawitz JW, Kalla P, Kirkman LK, Lang M, Leibowitz SG, Lewis DB, Marton J, McLaughlin DL, Raanan-Kiperwas H, Rains MC, Rains KC, Smith L. 2017. Enhancing protection for vulnerable waters. Nature Geoscience 10:809–815.

Downing JA. 2010. Emerging global role of small lakes and ponds: little things mean a lot. Limnetica 29:9–24.

Duvert C, Butman DE, Marx A, Ribolzi O, Hutley LB. 2018. CO_2 evasion along streams driven by groundwater inputs and geomorphic controls. Nature Geoscience 11:813–818.

Fenstermacher DE, Rabenhorst MC, Lang MW, McCarty GW, Needelman BA. 2014. Distribution, morphometry, and land use of Delmarva Bays. Wetlands 34:1219–1228.

Gleason RA, Tangen BA, Browne BA, Euliss NH Jr. 2009. Greenhouse gas flux from cropland and restored wetlands in the Prairie Pothole Region. Soil Biology and Biochemistry 41:2501–2507.

Grasset C, Mendonça R, Villamor Saucedo G, Bastviken D, Roland F, Sobek S. 2018. Large but variable methane production in anoxic freshwater sediment upon addition of allochthonous and autochthonous organic matter. Limnology & Oceanography 63:1488–1501.

Hassan M, Talbot J, Arsenault J, Martinez-Cruz K, Sepulveda-Jauregui A, Hoyos-Santillan J, Lapierre J. 2023. Linking dissolved organic matter to CO_2 and CH_4 concentrations in Canadian and Chilean peatland pools. Global Biogeochemical Cycles 37:e2023GB007715.

Holgerson MA. 2015. Drivers of carbon dioxide and methane supersaturation in small, temporary ponds. Biogeochemistry 124:305–318.

Holgerson MA, Raymond PA. 2016. Large contribution to inland water CO_2 and CH_4 emissions from very small ponds. Nature Geoscience 9:222–226.

Hondula KL, DeVries B, Jones CN, Palmer MA. 2021. Effects of using high resolution satellite-based inundation time series to estimate methane fluxes from forested wetlands. Geophysical Research Letters 48:e2021GL092556.

Hondula KL, Jones CN, Palmer MA. 2021b. Effects of seasonal inundation on methane fluxes from forested freshwater wetlands. Environmental Research Letters 16:084016.

Hotchkiss ER, Hall RO Jr, Sponseller RA, Butman D, Klaminder J, Laudon H, Rosvall M, Karlsson J. 2015. Sources of and processes controlling CO_2 emissions change with the size of streams and rivers. Nature Geoscience 8:696–699.

Jeffrey LC, Maher DT, Johnston SG, Kelaher BP, Steven A, Tait DR. 2019. Wetland methane emissions dominated by plant-mediated fluxes: Contrasting emissions pathways and seasons within a shallow freshwater subtropical wetland. Limnology & Oceanography 64:1895–1912.

Jones CN, Evenson GR, McLaughlin DL, Vanderhoof MK, Lang MW, McCarty GW, Golden HE, Lane CR, Alexander LC. 2018. Estimating restorable wetland water storage at landscape scales. Hydrological Processes 32:305–313.

Kifner LH, Calhoun AJK, Norton SA, Hoffmann KE, Amirbahman A. 2018. Methane and carbon dioxide dynamics within four vernal pools in Maine, USA. Biogeochemistry 139:275–291.

Koch S, Jurasinski G, Koebsch F, Koch M, Glatzel S. 2014. Spatial variability of annual estimates of methane emissions in a Phragmites Australis (Cav.) Trin. ex Steud dominated restored coastal brackish fen. Wetlands 34:593–602.

Kolka R, Trettin C, Tang W, Krauss K, Bansal S, Drexler J, Wickland K, Chimner R, Hogan D, Pindilli EJ, Benscoter B, Tangen B, Kane E, Bridgham S, Richardson C. 2018. Terrestrial wetlands. In: Second State of the Carbon Cycle Report (SOCCR2): A Sustained Assessment Report.

Kominoski JS, Pachón J, Brock JT, McVoy C, Malone SL. 2021. Understanding drivers of aquatic ecosystem metabolism in freshwater subtropical ridge and slough wetlands. Ecosphere 12:e03849.

Lane CR, Leibowitz SG, Autrey BC, LeDuc SD, Alexander LC. 2018. Hydrological, physical, and chemical functions and connectivity of non-floodplain wetlands to downstream waters: A review. Journal of the American Water Resources Association 54:346–371.

Lane CR, Creed IF, Golden HE, Leibowitz SG, Mushet DM, Rains MC, Wu Q, D'Amico E, Alexander LC, Ali GA, Basu NB,

Bennett MG, Christensen JR, Cohen MJ, Covino TP, DeVries B, Hill RA, Jencso K, Lang MW, McLaughlin DL, Rosenberry DO, Rover J, Vanderhoof MK. 2023. Vulnerable waters are essential to watershed resilience. Ecosystems 26:1–28.

Le PVV, Kumar P. 2014. Power law scaling of topographic depressions and their hydrologic connectivity. Geophysical Research Letters 41:1553–1559.

Lee S, McCarty GW, Moglen GE, Lang MW, Nathan Jones C, Palmer M, Yeo I-Y, Anderson M, Sadeghi AM, Rabenhorst MC. 2020. Seasonal drivers of geographically isolated wetland hydrology in a low-gradient, Coastal Plain landscape. Journal of Hydrology 583:124608.

Lee E, Epstein JM, Cohen MJ. 2023. Patterns of wetland hydrologic connectivity across coastal-plain wetlandscapes. Water Resources Research 59:e2023WR034553.

Li T, Canadell JG, Yang X-Q, Zhai P, Chao Q, Lu Y, Huang D, Sun W, Qin Z. 2022. Methane emissions from wetlands in China and their climate feedbacks in the 21st century. Environmental Science and Technology 56:12024–12035.

Limpert KE, Carnell PE, Trevathan-Tackett SM, Macreadie PI. 2020. Reducing emissions from degraded floodplain wetlands. Frontiers in Environmental Science 8:8.

Lindsay JB. 2016. Whitebox GAT: a case study in geomorphometric analysis. Computers & Geosciences 95:75–84. https://doi.org/10.1016/j.cageo.2016.07.003.

Liu L, Greaver TL. 2009. A review of nitrogen enrichment effects on three biogenic GHGs: the CO_2 sink may be largely offset by stimulated N_2O and CH_4 emission. Ecology Letters 12:1103–1117.

López Lloreda C, Maze J, Wardinski K, Corline N, McLaughlin D, Jones CN, Scott D, Palmer M, Hotchkiss ER. 2024. Dissolved CO_2 and CH_4 dynamics in Delmarva headwater wetlands, 2020–2022. https://portal.edirepository.org/nis/mapbrowse?packageid=edi.1601.1. Last accessed 15/03/2024

Lüdecke D, Ben-Shachar M, Patil I, Waggoner P, Makowski D. 2021. performance: An R Package for assessment, comparison and testing of statistical models. Journal of Open Source Software 6:3139.

Ludwig SM, Natali SM, Mann PJ, Schade JD, Holmes RM, Powell M, Fiske G, Commane R. 2022. Using machine learning to predict inland aquatic CO_2 and CH_4 concentrations and the effects of wildfires in the Yukon-Kuskokwim Delta Alaska. Global Biogeochemical Cycles 36:e2021GB007146.

Lupon A, Denfeld BA, Laudon H, Leach J, Karlsson J, Sponseller RA. 2019. Groundwater inflows control patterns and sources of greenhouse gas emissions from streams: Patterns and sources of stream C emissions. Limnology and Oceanography 64:1545–1557.

Maietta CE, Hondula KL, Jones CN, Palmer MA. 2020. Hydrological conditions influence soil and methane-cycling microbial populations in seasonally saturated wetlands. Frontiers in Environmental Science 8:593942.

Mao Y, Lin T, Li H, He R, Ye K, Yu W, He Q. 2024. Aerobic methane production by phytoplankton as an important methane source of aquatic ecosystems: Reconsidering the global methane budget. Science of the Total Environment 907:167864.

Marton JM, Creed IF, Lewis DB, Lane CR, Basu NB, Cohen MJ, Craft CB. 2015. Geographically isolated wetlands are important biogeochemical reactors on the landscape. BioScience 65:408–418.

Maryland Department of Information Technology Geographic Information Office. Digital Elevation Model of Queen Anne's County. https://lidar.geodata.md.gov/imap/rest/services. Last accessed 05/31/2021.

McDonough OT, Lang MW, Hosen JD, Palmer MA. 2015. Surface hydrologic connectivity between Delmarva Bay wetlands and nearby streams along a gradient of agricultural alteration. Wetlands 35:41–53.

McInerney E, Helton AM. 2016. The effects of soil moisture and emergent herbaceous vegetation on carbon emissions from constructed wetlands. Wetlands 36:275–284.

McLaughlin DL, Kaplan DA, Cohen MJ. 2014. A significant nexus: Geographically isolated wetlands influence landscape hydrology. Water Resources Research 50:7153–7166.

Mitsch WJ, Nahlik A, Wolski P, Bernal B, Zhang L, Ramberg L. 2010. Tropical wetlands: seasonal hydrologic pulsing, carbon sequestration, and methane emissions. Wetlands Ecology and Management 18:573–586.

Nikolenko O, Orban P, Jurado A, Morana C, Jamin P, Robert T, Knöller K, Borges AV, Brouyre S. 2019. Dynamics of greenhouse gases in groundwater: Hydrogeological and hydrogeochemical controls. Applied Geochemistry 105:31–44.

Peng S, Lin X, Thompson RL, Xi Y, Liu G, Hauglustaine D, Lan X, Poulter B, Ramonet M, Saunois M, Yin Y, Zhang Z, Zheng B, Ciais P. 2022. Wetland emission and atmospheric sink changes explain methane growth in 2020. Nature 612:477–482.

Peralta AL, Ludmer S, Matthews JW, Kent AD. 2014. Bacterial community response to changes in soil redox potential along a moisture gradient in restored wetlands. Ecological Engineering 73:302–306.

Phillips PJ, Shedlock RJ. 1993. Hydrology and chemistry of groundwater and seasonal ponds in the Atlantic Coastal Plain in Delaware, USA. Journal of Hydrology 141:157–178.

Pinheiro J, Bates D, R Core Team. 2023. nlme: Linear and nonlinear mixed effects models. R package version 3.1–163, https://CRAN.R-project.org/package=nlme.

R Core Team. 2020. R: a language and environment for statistical computing. R Foundation for Statistical Computing, Vienna, Austria. http://www.R-project.org/.

Rasilo T, Hutchins RHS, Ruiz-González C, Del Giorgio PA. 2017. Transport and transformation of soil-derived CO2, CH4 and DOC sustain CO2 supersaturation in small boreal streams. Science of the Total Environment 579:902–912.

Rennó CD, Nobre AD, Cuartas LA, Soares JV, Hodnett MG, Tomasella J, Waterloo MJ. 2008. HAND, a new terrain descriptor using SRTM-DEM: Mapping terra-firme rainforest environments in Amazonia. Remote Sensing of Environment 112:3469–3481.

Richardson DC, Holgerson MA, Farragher MJ, Hoffman KK, King KBS, Alfonso MB, Andersen MR, Cheruveil KS, Coleman KA, Farruggia MJ, Fernandez RL, Hondula KL, López Moreira Mazacotte GA, Paul K, Peierls BL, Rabaey JS, Sadro S, Sánchez ML, Smyth RL, Sweetman JN. 2022. A functional definition to distinguish ponds from lakes and wetlands. Scientific Reports 12:10472.

Rosentreter JA, Borges AV, Deemer BR, Holgerson MA, Liu S, Song C, Melack J, Raymond PA, Duarte CM, Allen GH, Olefeldt D, Poulter B, Battin TI, Eyre BD. 2021. Half of global methane emissions come from highly variable aquatic ecosystem sources. Nature Geoscience 14:225–230.

Rudolph JC, Arendt CA, Hounshell AG, Paerl HW, Osburn CL. 2020. Use of geospatial, hydrologic, and geochemical modeling to determine the influence of wetland-derived organic

matter in coastal waters in response to extreme weather events. Frontiers in Marine Science 7:18.

Saunois M, Stavert AR, Poulter B, Bousquet P, Canadell JG, Jackson RB, Raymond PA, Dlugokencky EJ, Houweling S, Patra PK, Ciais P, Arora VK, Bastviken D, Bergamaschi P, Blake DR, Brailsford G, Bruhwiler L, Carlson KM, Carrol M, Castaldi S, Chandra N, Crevoisier C, Crill PM, Covey K, Curry CL, Etiope G, Frankenberg C, Gedney N, Hegglin MI, Höglund-Isaksson L, Hugelius G, Ishizawa M, Ito A, Janssens-Maenhout G, Jensen KM, Joos F, Kleinen T, Krummel PB, Langenfelds RL, Laruelle GG, Liu L, Machida T, Maksyutov S, McDonald KC, McNorton J, Miller PA, Melton JR, Morino I, Müller J, Murguia-Flores F, Naik V, Niwa Y, Noce S, O'Doherty S, Parker RJ, Peng C, Peng S, Peters GP, Prigent C, Prinn R, Ramonet M, Regnier P, Riley WJ, Rosentreter JA, Segers A, Simpson IJ, Shi H, Smith SJ, Steele LP, Thornton BF, Tian H, Tohjima Y, Tubiello FN, Tsuruta A, Viovy N, Voulgarakis A, Weber TS, van Weele M, van der Werf GR, Weiss RF, Worthy D, Wunch D, Yin Y, Yoshida Y, Zhang W, Zhang Z, Zhao Y, Zheng B, Zhu Q, Zhu Q, Zhuang Q. 2020. The global methane budget 2000–2017. Earth Systems Science Data 12:1561–1623.

Savenije HHG. 2010. Topography driven conceptual modelling (FLEX-Topo). Hydrol Earth Syst Sci 14:2681–2692.

Sharp SJ, Maietta CE, Stewart GA, Taylor AK, Williams MR, Palmer MA. 2024. Net methane production predicted by patch characteristics in a freshwater wetland. Journal of Geophysical Research Biogeosciences 129:e2023JG007814.

Stewart GA, Kottkamp AI, Williams MR, Palmer MA. 2023. Setting a reference for wetland carbon: the importance of accounting for hydrology, topography, and natural variability. Environmental Research Letters 18:064014.

Tiner RW. 2003. Geographically isolated wetlands of the United States. Wetlands 23:494–516.

Wang Z, Sadat-Noori M, Glamore W. 2022. Groundwater discharge drives water quality and greenhouse gas emissions in a tidal wetland. Water Science and Engineering 15:141–151.

Ward ND, Bianchi TS, Martin JB, Quintero CJ, Sawakuchi HO, Cohen MJ. 2020. Pathways for methane emissions and oxidation that influence the net carbon balance of a subtropical cypress swamp. Frontiers in Earth Science 8:573357.

Wardinski KM, Hotchkiss ER, Jones CN, McLaughlin DL, Strahm BD, Scott DT. 2022. Water-soluble organic matter from soils at the terrestrial-aquatic interface in wetland-dominated landscapes. Journal of Geophysical Research Biogeosciences 127:e2022JG006994.

Webb JR, Santos IR, Tait DR, Sippo JZ, Macdonald BCT, Robson B, Maher DT. 2016. Divergent drivers of carbon dioxide and methane dynamics in an agricultural coastal floodplain: Post-flood hydrological and biological drivers. Chemical Geology 440:313–325.

Webb JR, Santos IR, Maher DT, Finlay K. 2019. The importance of aquatic carbon fluxes in net ecosystem carbon budgets: A catchment-scale review. Ecosystems 22:508–527.

Wickham H. 2016. ggplot2: Elegant graphics for data analysis. New York: Springer-Verlag.

Wu Q, Lane CR, Wang L, Vanderhoof MK, Christensen JR, Liu H. 2019. Efficient delineation of nested depression hierarchy in digital elevation models for hydrological analysis using level-set method. Journal of the American Water Resources Association 55:354–368.

Wu Q, Brown A. 2022. whitebox: 'WhiteboxTools' R Frontend. R package version 2.2.0. https://CRAN.R-project.org/package=whitebox

Yvon-Durocher G, Allen AP, Bastviken D, Conrad R, Gudasz C, St-Pierre A, Thanh-Duc N, Del Giorgio PA. 2014. Methane fluxes show consistent temperature dependence across microbial to ecosystem scales. Nature 507:488–491.

Zhu Y, Purdy KJ, Martínez Rodríguez A, Trimmer M. 2023. A rationale for higher ratios of CH_4 to CO_2 production in warmer anoxic freshwater sediments and soils. Limnology and Oceanography Letters 8:398–405.